Expert Opinion

Radiotargeting agents for cancer therapy

Amin I Kassis
Harvard Medical School, Department of Radiology, Armenise Building, 200 Longwood Avenue, Boston, MA 02115, USA

Although the general radiobiological principles underlying external beam therapy and radionuclide therapy are the same, there are significant differences in the radiobiological effects observed in mammalian cells. In external beam therapy and brachytherapy, emissions are composed of photons, whereas in radionuclide therapy, the radiations of interest are particulate. This article will explore the special features that characterise the biological effects consequent to the traversal of charged particles through mammalian cells. In addition, it will highlight what has been learned when these radionuclides and targeting radiopharmaceuticals are used to treat cancers.

Keywords: α-particle emitter, β-particle emitter, Auger-electron emitter, radiobiology, radionuclide therapy

Expert Opin. Drug Deliv. (2005) 2(6):981-991

1. Introduction

For many years, the scientific and medical communities have used radionuclides for therapy, and sealed sources, such as radium needles and capsules, are now commonplace. However, with the exception of a relatively select number of applications (e.g., high doses of 131-iodine for the therapy of certain thyroid tumours), the hopes for employing unsealed sources are still mainly unrealised. The problem has three components: the first is the availability of radionuclides with appropriate physical properties; the second involves the interaction between the radionuclide and its biological environment (i.e., the radiation biology of the decay product); and the third is the identification of a suitable carrier molecule with which to bring the radionuclide into the vicinity of the targeted tissue (e.g., cancerous cells). The development of effective radionuclide therapy requires knowledge of all these elements. In the case of the radionuclide, one must consider its mode of decay, including the nature of the particulate radiations and their energies, its physical half-life, and its chemistry in relation to the carrier molecule. In the case of the carrier, one must define its stability and specificity, the biological mechanisms that will bind it to the targeted cells, including the number of accessible sites and the affinity of the carrier to these sites, the stability of the receptor–carrier molecule complex, the distribution of the sites among cells (both target and nontarget), the relationship of site appearance to the cell cycle, and the microenvironment of the target (for a tumour, its vascularity, vascular permeability, oxygenation, microscopic organisation and architecture, including the mobility of the cells, their location, and their accessibility to intralymphatic, intraperitoneal, intracerebral and intramedullary pathways). In addition, the outcome is dependent on certain biological responses that are outlined in Section 3.

This introductory article will emphasise both the special features that characterise the biological effects consequent to the traversal of charged particles through mammalian cells and the current state of knowledge concerning the use of these radionuclides to treat cancers.

Ashley Publications
www.ashley-pub.com

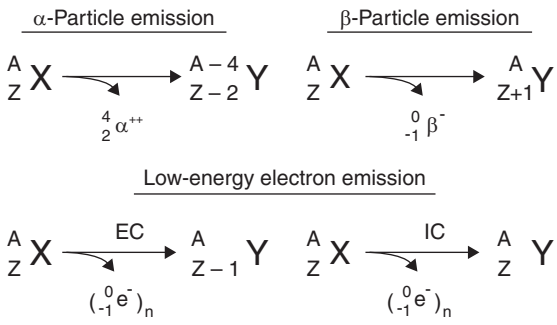

Figure 1. Schematic figure of emissions produced during decay of therapeutic radionuclides.
EC: Electron capture; IC: Internal conversion.

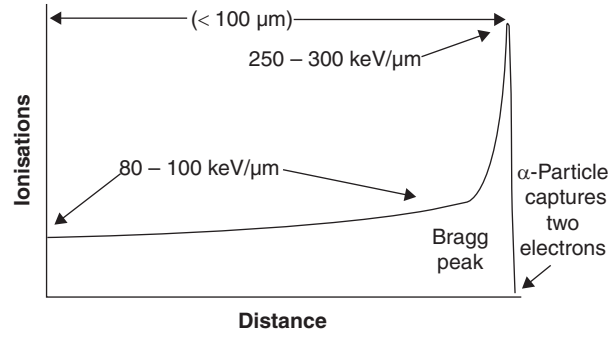

Figure 2. Ionisation density along the α-particle track as function of traversed distance.

2. Therapeutic radionuclides

In general, the distribution of therapeutic radiopharmaceuticals throughout a targeted solid tumour is not homogeneous, mainly as a result of the inability of the radiolabelled molecules to penetrate evenly dissimilar regions within a solid tumour mass, the interstitial pressure of the tumour, or differences in the specific binding-site densities of individual tumour cells. Such nonuniformity will lead to dosimetric nonhomogeneities (i.e., major differences in the absorbed doses to individual tumour cells), especially in the case of radiopharmaceuticals labelled with α-particle and nonenergetic β-particle emitters. Consequently, the mean absorbed dose is not necessarily a good predictor of radiotherapeutic efficacy.

2.1 Energetic particles

2.1.1 α-Particle emitters

Over the past 30 years, the therapeutic potential of several α-particle-emitting radionuclides has been assessed. These particles are positively charged with a mass and charge equal to that of the helium nucleus, and their emission leads to a daughter nucleus that has two fewer protons and two fewer neutrons (Figure 1). They have energies of 5 – 9 MeV and corresponding tissue ranges of 5 – 10 cell diameters (Table 1) and travel in straight lines. The linear energy transfer (LET), in keV/μm, which reflects energy deposition and, therefore, ionisation density along the track of these energetic, heavy and doubly charged (+2) particles is very high (~ 80 – 100 keV/μm) throughout most of their ≤ 100 μm path before increasing to ~ 300 keV/μm toward the end of the track (Bragg peak) (Figure 2). Consequently, in the case of cell self-irradiation, the following two factors must be considered when evaluating the therapeutic efficacy of α-particle emitters: distance of the decaying atom from the targeted mammalian cell nucleus in relation to the probability of a nuclear traversal (Figure 3), and the contribution of heavy ion recoil of the daughter atom, in particular when the α-particle emitter is covalently bound to nuclear DNA [1]. Of equal importance is the magnitude of cross-dose (from radioactive sources associated with one cell to an adjacent/nearby cell; see Section 7) as this will vary considerably depending on the size of the labelled cell cluster, the fraction of cells labelled [2] and the distance from the nucleus to be traversed (Figure 3).

2.1.2 β-Particle emitters

Current radionuclide therapy in humans is based almost exclusively on energetic β-particle-emitting isotopes. β-Particles are negatively charged electrons, emitted from the nucleus of a decaying radioactive atom (1 electron/decay), that have various energies (zero up to a maximum) and, thus, a distribution of ranges (Table 1). After their emission, the daughter nucleus has one more proton and one less neutron (Figure 1). As these β-particles traverse matter, they lose their kinetic energies and eventually follow a contorted path and come to a stop. Because of their small mass, the recoil energy of the daughter nucleus is negligible. In addition, the LET of these energetic, light and negatively charged (-1) particles is very low (~ 0.2 keV/μm) along their ≤ 1 cm path (i.e., they are sparsely ionising), except for the few nanometres at the end of the range (Figure 4). Consequently, their use as therapeutic agents predicates the presence of very high radionuclide concentrations within the targeted tissue. An important implication of the long range of each emitted electron is the production of cross-fire, a circumstance that negates the need to target every cell within the tumour. As with α-particles, the probability of the emitted β-particle traversing the targeted cell nucleus depends to a large degree on the position of the decaying atom in relation to the nucleus (specifically nuclear DNA) of the targeted tumour cell, its distance from the tumour cell nucleus, and the radius of the latter (Figure 3). Obviously, intranuclear localisation of therapeutic radiopharmaceuticals is highly advantageous and, if possible, should always be sought.

2.2 Nonenergetic particles

During the decay of certain radioactive atoms, a vacancy is formed (most commonly in the K shell) as a consequence of

Table 1. General characteristics of therapeutic radionuclides.

Decay	Particles (#)*	E_{min} – E_{max}	Range	LET
β^--particle	Energetic electrons (1)	50 – 2300 keV‡	0.05 – 12 mm	~ 0.2 keV/µm
α^{++}-particle	He nuclei (1)	5 – 9 MeV§	40 – 100 µm	~ 80 keV/µm
EC/IC	Nonenergetic electrons (5 – 30)	eV – keV§	2 – 500 nm	~ 4 – 26 keV/µm

*Number of particles emitted per decaying atom. ‡Average (> 1% intensity); continuous distribution of energy. §Monoenergetic.
EC: Electron capture; E_{max}: Maximum electron energy; E_{min}: Minimum electron energy; IC: Internal conversion; LET: Linear energy transfer.

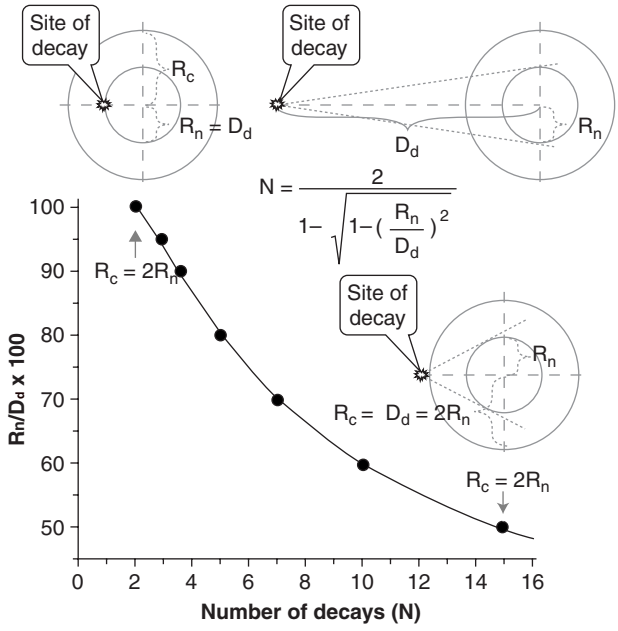

Figure 3. Number of radioactive atoms required to ensure traversal of the cell nucleus by one energetic particle, as function of distance from the centre of the cell. Nuclear radius to distance of decaying atom (%) is plotted as function of number of decays. When decaying atoms are on nuclear membrane at least two radioactive atoms are needed for one nuclear traversal; when decaying atoms are localised on cell membrane and diameter of cell is twice that of nucleus, > 15 radioactive atoms are necessary to insure one nuclear traversal. Nuclear localisation of radioactive atom is the only condition that will lead to one traversal per decaying atom.
D_d: Distance of decaying atom from centre of cell for one nuclear traversal (this must be less than the particle range; R_c: Cell radius; R_n: Nucleus radius.

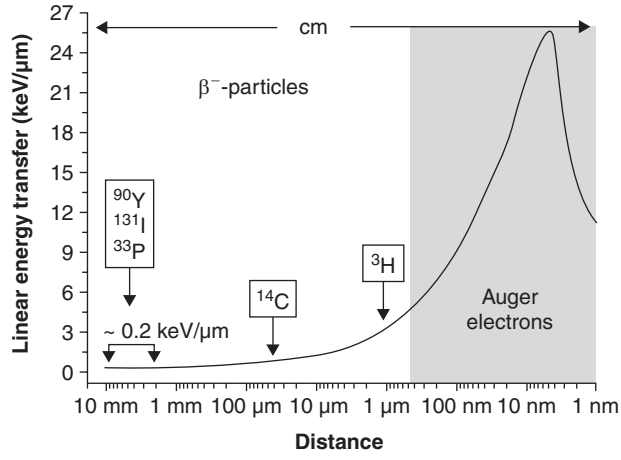

Figure 4. Linear energy transfer, reflecting ionisation density as function of distance, along tracks of energetic β-particles and Auger electrons.

electron capture (EC) and/or internal conversion (IC). Such vacancies are rapidly filled by electrons dropping in from higher shells. This process leads to a cascade of atomic electron transitions that moves the vacancy toward the outermost shell. Each inner-shell electron transition results in the emission of a characteristic X-ray photon or an Auger, Coster-Kronig, or super Coster-Kronig monoenergetic electron (collectively called Auger electrons). Typically, an atom undergoing EC and/or IC emits, on average, 5 – 30 Auger electrons with energies ranging from a few eV to ~ 1 keV (Table 1). In addition to low-energy electrons, this form of decay leaves the daughter atom with a high positive charge resulting in subsequent charge-transfer processes. The very low energies of Auger electrons have two major consequences: first, these light, negatively charged (-1) particles travel in contorted paths and their range in water is from a fraction of a nanometre up to ~ 0.5 µm (Table 1); and second, multiple ionisations (LET 4 – 26 keV/µm) occur in the immediate vicinity (few nanometres) of the decay site (Figure 4), reminiscent of those observed along the path of an α-particle [3,4]. Finally, the short range of Auger electrons necessitates their close proximity to the radiosensitive target (DNA) for radiotherapeutic effectiveness. This is essentially a consequence of the precipitous drop in energy density as a function of distance in nanometres [5-7].

3. Radiobiological effects

The deposition of energy by ionising radiation is a random process. The energy absorbed by cells can induce certain molecular modifications that may lead to cell death. Despite the fact that this process is stochastic in nature, the death of a few cells, in general, within a tissue or an organ will not have a

significant effect. As the dose increases, more cells will die with the eventual impairment of organ/tissue function.

3.1 Molecular lesions

DNA is generally agreed to be the principal target responsible for the biological effects of ionising radiation. A number of different lesions are produced (e.g., single-strand breaks, double-strand breaks [DSBs], base damage, DNA–protein crosslinks and multiply damaged sites). In general, these are repaired with high fidelity, the exceptions being DSB and multiply damaged sites. The lesions may be produced by the direct ionisation of DNA (direct effect) or by the interaction of free radicals (mostly hydroxyl radicals produced in water molecules that diffuse a few nanometres) with DNA.

The distribution of ionisations within the DNA structure and the type of lesion created depend on the nature of the incident particle and its energy. α-Particles produce a high density along a linear path; energetic β-particles, infrequent ionisations along a linear path; low-energy electrons, frequent ionisations along an irregular path; and Auger cascades, clusters of high ionisation density. DSBs generated by high specific ionisation (α-particles and Auger-electron cascades) are less reparable than those created by more sparsely ionising radiation.

3.2 Cellular responses

3.2.1 *Clonal survival*

When mammalian cells are irradiated by particle(s) emitted from a decaying radionuclide within a radiopharmaceutical, a certain fraction of the cells will lose their capacity to divide indefinitely (i.e., they will fail to give rise to a clone of similar cells). Several *in vitro* assays have been described that measure the ability of cells to proliferate. In practice, these assays measure the capacity of cells to reproduce successfully and, thus, to form a colony. Using a colony-forming assay, it is possible to determine the decrease in survival, expressed as a surviving fraction, as a function of a graded radiation dose.

Radiation survival curves are log–linear plots of surviving fraction (log) versus dose (linear). The shape of the curve constructed through such a set of survival points varies and will depend on certain biological, physical and chemical factors. In general, two types of dose–survival curves have been described (Figure 5). For the exponential survival curve, the slope is always constant and can be expressed by Equation 1, where S/S_0 is the surviving fraction of the irradiated cells, D is the dose delivered and D_0 is the dose needed to reduce survival to 0.37. This type of survival curve is observed when mammalian cells are exposed to high-LET radiation (e.g., α-particle emissions, DNA-incorporated Auger-electron emitters).

$$S/S_0 = e^{-\frac{D}{D_0}} \qquad (1)$$

In the second type of dose–response relationship, expressed by the sigmoidal survival curve (Figure 5), the efficiency of cell kill is not constant: at low doses, a slow decrease in survival is observed and the curve has a shoulder; at higher doses, an exponential decrease in survival is seen. The linear–quadratic equation for fitting this curve is Equation 2, where α equals the rate of cell kill by a single-hit mechanism, D is the dose delivered and β equals the rate of cell kill by a double-hit mechanism. This type of survival curve is routinely seen when mammalian cells are exposed to low-LET radiation (e.g., X-rays, energetic β-particles, extranuclear Auger electrons). If radiation is protracted or the dose rate is low, as often occurs with radionuclides, the α-term predominates. It is important to note that the α:β ratio is the dose at which cell killing by the linear and quadratic components is equal.

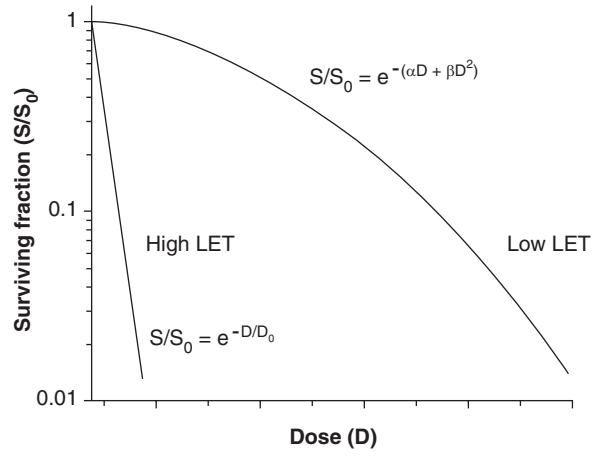

Figure 5. Survival of mammalian cells after high- and low-LET irradiation. With high-LET radiation (α-particles and nonenergetic electrons) curve shows exponential decrease in survival, and with low-LET radiation (energetic electrons), curve exhibits a shoulder.
α: Rate of cell kill by a single-hit mechanism; β: Rate of cell kill by a double-hit mechanism; LET: Linear energy transfer; S/S_0: Surviving fraction of the irradiated cells.

$$S/S_0 = e^{-(\alpha D + \beta D^2)} \qquad (2)$$

Although it is clear that pharmaceuticals labelled with radionuclides whose decay results in a purely exponential decrease in cell survival (with every decay leading to a corresponding decrease in survival [Equation 1]) are preferable for radiotherapy, the exponential nature of both types of survival curve has important implications. In essence, it indicates that only very high doses will reduce the number of viable cancer cells in a macroscopic tumour to less than one, and that no dose will be large enough to eradicate with 100% certainty the clonogenic cells, especially as the magnitude of the dose will always be limited by normal tissue tolerance.

3.2.2 *Division delay and programmed cell death*

After irradiation, delay in the progression of dividing cells through their cell cycle is a well-documented phenomenon. It

is reversible and its length is dose dependent. The delay occurs only at specific points in the cell cycle and is similar for both surviving and nonsurviving cells: cells in premitotic G_2 of the cell cycle show maximum delay, cells in G_1 have little delay, those in S phase display a moderate delay, and cells in mitosis continue through division mainly undisturbed.

Division delay allows irradiated cells time to determine their fate. When cells are irradiated and DNA is damaged, the damage is sensed and various genes are activated. Cells held at checkpoints await the repair of DNA, and then proceed through the cell cycle. Alternatively, damage may be nonreparable and the cells are induced to undergo programmed cell death or apoptosis. The apoptotic pathways are under tight genetic regulation with the tumour suppressor gene *p53* playing a central role. Cellular responses are variable and require the action of certain proteolytic caspases. Lymphoid tumour cells are more likely to undergo apoptosis than epithelial cells, which may account for the success of radioimmunotherapy in certain lymphomas. In epithelial cells, apoptosis seems to account for only a small portion of clonal cell death.

3.2.3 Oxygen enhancement ratios

Oxygen radiosensitises mammalian cells to the damaging effects of radiation. Consequently, hypoxic cells can be up to threefold more radioresistant than well-oxygenated cells. It is thought that following cell irradiation, oxygen enhances free radical formation and/or blocks reversible and reparable chemical alterations. The oxygen effect is maximal for low-ionisation-density radiation (high-energy β-particles) and minimal for high-LET radiation (α-particles, low-energy electrons including Auger-electron cascades).

3.2.4 Bystander effect

The term 'bystander effect' is applied to the biological responses of cells that neighbour irradiated cells but have not been irradiated themselves. Increased mutation rates and decreased survival rates have been reported. Originally observed with external α-particle beams *in vitro*, the phenomenon has been observed in subcutaneous tumours [8]. These observations have negated a central tenet of radiobiology that damage to cells is caused only by direct ionisations and/or free radicals generated as a consequence of the deposition of energy within the nuclei of mammalian cells. The importance of the bystander effect as an enhancer of radiotherapeutic efficacy is yet to be determined.

3.2.5 Self-dose, cross-fire and nonuniform dose distribution

When radionuclides are employed for therapy, cells may be irradiated by decays taking place on or within the targeted cells (self-dose) or in neighbouring or distant cells (cross-fire). Because of geometric factors associated with linear paths, the self-dose from energetic α- and β-particles is very dependent on their position on or within the tumour cell, whereas that for Auger-electron emitters depends on the proximity of the decaying atom to DNA.

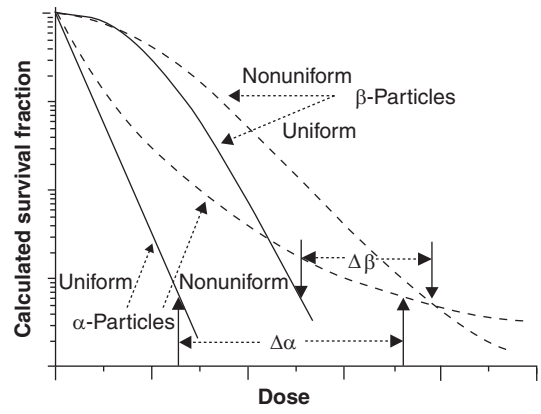

Figure 6. Schematic representation of relationship between mammalian cell survival and radionuclide distribution as a function of dose. Curves for uniform (solid lines) and nonuniform (broken lines) α- and β-particles irradiation.

In targeted radionuclide therapy, the distribution of radioactivity and, hence, the absorbed dose tend to be nonuniform. Consequently, higher doses are required to sterilise the targeted cells. Using mathematical modeling, Humm has calculated that the difference in dose needed for a similar decrease in survival fraction with uniform and nonuniform dose distributions of α-particle-emitting radionuclides is greater than that for energetic β-particles (i.e., $\Delta\alpha > \Delta\beta$) (Figure 6) [9]. O'Donoghue has also described a mathematical model that examines the impact of dose nonuniformity, as well as dose rate, on therapeutic response [10]. This model predicts that as the absorbed dose distribution becomes less uniform, the surviving fraction increases for any mean absorbed dose; a nonuniform dose distribution grows proportionately less effective as the absorbed dose increases; and the difference in survival fraction resulting from uniform versus nonuniform doses is more pronounced as the radiosensitivity of tumour cells increases.

3.2.6 Half-life

Because many biological responses to radiation are sensitive to dose rate as well as total dose, the physical half-life ($T_{1/2P}$) of the radionuclide employed and the tumour and normal tissue residence half-life ($T_{1/2B}$) can be of consequence. For a radiopharmaceutical with an infinite residence time in a tumour or tissue, a radionuclide with a long physical half-life will deliver more decays than one with a short half-life if both have the same initial radioactivity. Moreover, there can be a striking difference in the time-dependent dose rate delivered by the two. If the number of radionuclide atoms per unit of tissue mass is n and the energy emitted (and absorbed) per decay is E, then the absorbed-dose rate is proportional to $nE{:}T$ where T is the half-life. The ratio $E{:}T$ is an important indicator of the intrinsic radiotherapeutic potency of the radionuclide [11]. In general,

for biological reasons, higher dose rates delivered over shorter treatment times are more effective than lower dose rates delivered over longer periods. Thus, a radionuclide with a shorter half-life will tend to be more biologically effective than one with a similar emission energy but longer half-life. For example, when the same number of 125-iodine and 123-iodine atoms (covalently conjugated to a tumour-targeting agent) is bound to a tumour, their relative effectiveness depends on the tumour doubling time and the rate at which the radiopharmaceutical dissociates from the target. When both factors are very long, the longer-lived 125-iodine ($T_{1/2}$ 60 days) is theoretically more effective; otherwise the shorter-lived 123-iodine ($T_{1/2}$ 13.3 h) is preferred.

4. Choice of vector or ligand

The choice of chemical carrier in cancer therapy is of equal importance to that of the radionuclide. It is the properties of the former on which targeted therapy depends. The selection of a suitable carrier molecule rests on many factors, including biological specificity and *in vivo* stability, the mechanism(s) that lead to its binding to the targeted cells and the affinity of the carrier for the binding sites, and the stability of the receptor–carrier complex thus formed. Obviously, the chemical properties of the carrier molecule must enable the conjugation of a therapeutic radionuclide without degradation of the intrinsic characteristics of the molecule.

5. Properties of targets

Important factors in the case of tumours are their accessibility, the number of binding sites, the distribution of binding sites among the targeted and nontargeted cells, and the expression of these binding sites during each phase of the cell cycle. The microscopic environment of the target, including tumour vascularity, vascular permeability, oxygenation, as well as its microscopic organisation and architecture, is also extremely important [12,13].

To optimally target a radiopharmaceutical, the route of administration (e.g., intravenous, intralymphatic, intraperitoneal, intracerebral, intravesical, intrathecal and intrasynovial) must also be considered. Some pathways may provide a mechanical means for maximising tumour:nontumour ratios.

Finally, specific activity of the radiopharmaceutical (fraction of targeting molecules that are tagged with radioactive atoms) should be taken into account, especially when receptors can be saturated easily and, therefore, weaker binding nonspecifically to nontargeted cells can compete with the target. It should be noted that certain treatments are sometimes assisted by a mass effect (e.g., tumour uptake of radiolabelled antibodies can be enhanced by the addition of unlabelled immunoglobulin).

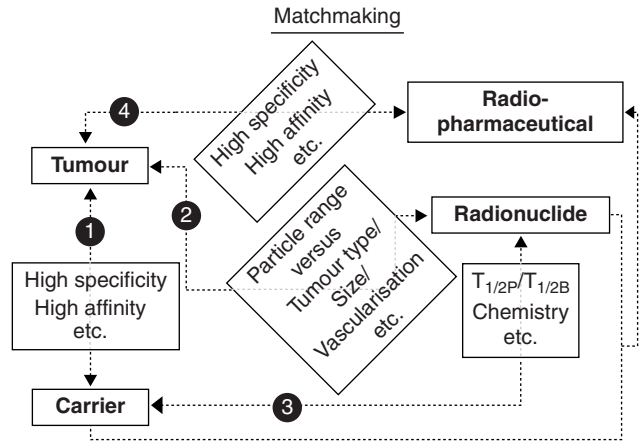

Figure 7. Matchmaking of tumour, radionuclide, targeting ligand and radiopharmaceutical.
$T_{1/2B}$: Biological half-life; $T_{1/2P}$: Physical half-life.

6. Characteristics of an ideal therapeutic radiopharmaceutical

The successful development of a therapeutic radiopharmaceutical necessitates the multistep matching of the disease and the carrier molecule, the disease and the radionuclide, the carrier and the radionuclide, and the radiopharmaceutical and the disease (Figure 7). During these successive steps, special attention must be paid to insure the compatibility of the individual components. Under ideal conditions, a therapeutic radiopharmaceutical would be characterised by:

- very high specificity for tumour cells
- high affinity to tumour cells
- stability in blood *in vivo* (not catabolised/metabolised; if somewhat unstable, metabolism/catabolism half-life should be much greater than $T_{1/2P}$ of the radionuclide)
- $T_{1/2B}$ comparable with $T_{1/2P}$ of the radionuclide
- rapid targeting of tumour cells
- significant retention by tumour cells for a period two- to threefold longer than the $T_{1/2P}$ of the radionuclide
- lack of catabolism by tumour cells
- minimal take up and retention by normal tissues/cells
- rapid excretion from the body
- pharmacokinetics not altered by repeated injection
- efficient cell killing (i.e., high ionisation densities in DNA)
- Radionuclide distribution within tumour cell clusters less heterogenous than the range of emitted particles
- deposition of a therapeutic dose in all tumour cells
- delivery of a toxic dose to tumour cells prior to deposition of the maximum tolerated dose in normal tissues
- irradiation leading to cell death only (i.e., no other radiation-induced biological effects such as mutations and transformations).

Table 2. α-Particle emitters: physical properties.

Radionuclide	E_{av} (MeV)*	R_{av} (μm)‡	Half-life
^{211}At	6.79	60	7.2 h
^{212}Bi	7.80	75	61 min
^{213}Bi	8.32	84	46 min
^{223}Ra	5.64	45	11.43 days
^{225}Ac	6.83	61	10 days

*Mean energy of α-particles emitted per disintegration [12]. ‡Mean range of α-particles calculated using second-order polynomial regression fit (data from [13]): $R = 3.87E + 0.75E^2 - 0.45$, where R is the range (μm) in unit density matter and E is the α-particle energy (MeV).

Table 3. β-Particle emitters: physical characteristics.

Radionuclide	Half-life	$E_{\beta\text{- (max)}}$ (keV)*	$R_{\beta\text{- (max)}}$ (mm)‡
^{33}P	25.4 days	249	0.63
^{177}Lu	6.7 days	497	1.8
^{67}Cu	61.9 h	575	2.1
^{131}I	8.0 days	606	2.3
^{186}Re	3.8 days	1077	4.8
^{165}Dy	2.3 h	1285	5.9
^{89}Sr	50.5 days	1491	7.0
^{32}P	14.3 days	1710	8.2
^{166}Ho	28.8 h	1854	9.0
^{188}Re	17.0 h	2120	10.4
^{90}Y	64.1 h	2284	11.3

*Maximum energy of β-particles emitted per disintegration. ‡Range (μm) for electrons with E = 0.02 – 100 keV calculated using Cole's equation [4]: $R = 0.043(E + 0.367)^{1.77} - 0.007$, whereas range (mm) for electrons with E (MeV) calculated using second order fits (data from [22]):
$R_{(0.1 - 0.5\ MeV)} = 2.4E + 2.86E^2 - 0.14$,
and $R_{(0.5 - 2.5\ MeV)} = 5.3E + 0.0034E^2 - 0.93$.

7. Experimental therapeutics

7.1 Energetic particles

7.1.1 α-Emitters

The application of α-particle-emitting radionuclides as targeted therapeutic agents continues to be of interest. When such radionuclides are selectively accumulated in the targeted tissues (e.g., tumours), their decay should result in highly localised energy deposition in the tumour cells and minimal irradiation of surrounding normal host tissues.

The investigation of the therapeutic potential of α-particle emitters has focused mainly on five radionuclides: 211-astatine (^{211}At), 212-bismuth (^{212}Bi), 213-bismuth (^{213}Bi), 223-radium (^{223}Ra) and 225-actinium (^{225}Ac) (Table 2). *In vitro* studies [14,15] have demonstrated that the decrease in mammalian cell survival after exposure to uniformly distributed α-particles from such radionuclides is monoexponential

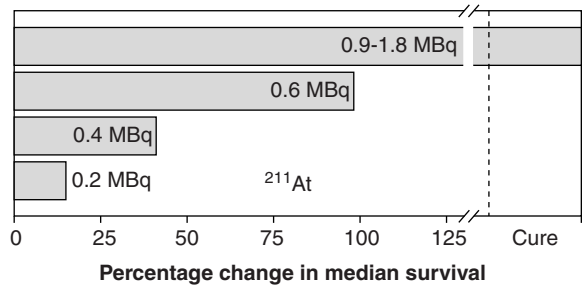

Figure 8. Percentage change in median survival of ovarian-cancer-bearing mice treated with α-particle-emitting radiocolloid [16].

but that, as predicted theoretically [9] and shown experimentally [1] after the decay of ^{211}At-labelled 5-astato-2′-deoxyuridine ([^{211}At]UdR), these curves develop a tail when the dose is nonuniform (Figure 6). Such studies have also indicated that the traversal of one-to-four α-particles through a mammalian cell nucleus will kill the cell [1,14,15]. In comparison, because the LET of negatrons emitted by the decay of energetic β-emitters is ~ 0.2 keV/μm (Figure 4), thousands of β-particles must traverse a cell nucleus for its sterilisation.

Investigators have also assessed the therapeutic potential of α-particle emitters in tumour-bearing animals [16-19]. Bloomer and colleagues [16] have reported a dose-related prolongation in median survival when mice bearing an intraperitoneal murine ovarian tumour are treated with [^{211}At]tellurium colloid administered directly into the peritoneal cavity. Whereas this α-particle-emitting radiocolloid is curative without serious morbidity (Figure 8), β-particle-emitting radiocolloids (32-phosphorus, 165-dysprosium, 90-yttrium [^{90}Y]) are much less efficacious. In another set of *in vivo* studies examining the therapeutic efficacy of a ^{212}Bi-labelled monoclonal antibody, the radionuclide is most effective when used with a carrier that entails target specificity [17]. Finally, a recent report by McDevitt and colleagues [19] has demonstrated that ^{225}Ac-labelled internalising antibodies are therapeutically effective in mice bearing solid prostate carcinoma or disseminated lymphoma.

7.1.2 β-Emitters

Radionuclide-based tumour therapy has been carried out mainly with β-particle emitters. Findings indicate that the exposure of cells *in vitro* to β-particles leads, in general, to survival curves that have a distinct shoulder and a D_0 of several thousand decays [20,21]. Despite the rather low *in vitro* toxicity, these radionuclides continue to be pursued for targeted therapy. This is due, to a great extent, to the availability and favourable characteristics of many energetic β-particle-emitting isotopes (Table 3), including the irradiation of cells within the longer range (mm – cm) of the emitted electron particles (i.e., cross-fire). As mentioned above, the main advantage of cross-fire is that it negates the necessity of the radiotherapeutic

Table 4. Auger-electron emitters: physical properties.

Radionuclide (#)*	Half-life	Total electron yield per decay		
		Long-range electrons (%)	*Short-range electrons (%)*	*Very short-range electrons (%)*
^{125}I (20)	60.5 days	20 (98%)	18 (86%)	8 (39%)
^{123}I (11)	13.3 h	11 (98%)	10 (89%)	5 (40%)
^{77}Br (7)	57 h	7 (100%)	6 (95%)	3 (51%)
^{111}In (15)	3 days	15 (98%)	14 (91%)	8 (53%)
^{195m}Pt (36)	4 days	33 (92%)	33 (79%)	7 (19%)
	Range	< 0.5 µm	< 100 nm	< 2 nm
	LET‡	4 – 26	9 – 26	< 18

*Average number of electrons emitted per decay. ‡Fit of data by Cole [4].
LET: Linear energy transfer.

agent's being present within each of the targeted cells (i.e., it counteracts a certain degree of heterogeneity). However, to deliver an effective therapeutic dose to the targeted tissue, the following conditions must be met: the radiotherapeutic agent must concentrate within foci throughout the targeted tumour mass; the distances between these foci must be equal to or less than twice the maximum range of the emitted energetic β-particles; the concentration of the radiotherapeutic agent within each focus must be sufficiently high to produce a cumulative cross-fire dose of ≥ 10,000 cGy to the surrounding targeted cells. As dose is inversely proportional to the square of distance, the concentration of the therapeutic agent needed to deposit such cytocidal doses rises many fold when the distance between the radioactive foci increases.

Experimentally, these predictions have been substantiated in various animal-tumour therapy studies. Investigators have assessed the therapeutic efficacy of ^{131}I-labelled monoclonal antibodies in rodents bearing subcutaneous tumours. Although a substantial proportion of cells within a tumour mass shows reduced/no expression of the targeted antigen and, therefore, is not targeted by the radioiodinated antibody, ^{131}I-labelled antibodies that localise in high concentrations in tumours are therapeutically efficacious and can lead to total tumour eradication [22]. Thus, even when 131-iodine is not-so-uniformly distributed within a tumour, the decay of this radionuclide can lead to the sterilisation of small tumours in mice so long as it is present in sufficiently high concentrations. Similar results have been reported with radiopharmaceuticals labelled with other β-particle-emitting isotopes, in particular ^{90}Y [23-25] and 67-copper [26]. An important outcome of these findings has been the recent successful introduction of ^{131}I- and ^{90}Y-labelled antibodies in the clinic [27-29].

7.2 Nonenergetic particles

The therapeutic potential of radionuclides that decay by EC and/or IC has, for the most part, been established with 125-iodine. Studies with this and other Auger-electron-emitting radionuclides (Table 4) have shown that multiple electrons are emitted per decaying atom; the distances traversed by these electrons are mainly in the nanometre range; the LET of the electrons is > 20-fold higher than that observed along the tracks of energetic (> 50 keV) β-particles; and many of the emitted electrons dissipate their energy in the immediate vicinity of the decaying atom and deposit 10^6 – 10^9 rad/decay within a few-nanometre sphere around the decay site [5,6,30-34]. From a radiobiologic prospective, the tridimensional organisation of chromatin within the mammalian cell nucleus involves many structural level compactions (nucleosome, 30-nm chromatin fibre, chromonema fibre, and so on) whose dimensions are within the range of these high-LET (4 – 26 keV/µm), low-energy (≤ 1.6 keV), short-range (≤ 150 nm) electrons. Therefore, the toxicity of Auger-emitting radionuclides is expected to be quite high and to depend critically on close proximity of the decaying atom to DNA. These predictions have been substantiated by *in vitro* studies, which have indicated that the decay of Auger-electron emitters covalently bound to nuclear DNA leads to a monoexponential decrease in survival [6,32,35]; the curves may or may not exhibit a shoulder when the decaying atoms are not covalently bound to nuclear DNA [33,36,37]; and, in general, intranuclear decay accumulation is highly toxic (D_0 ~ 100 – 500 decays/cell), whereas decay within the cytoplasm or extracellularly produces no extraordinary lethal effects and these survival curves resemble those observed with X-ray (have a distinct shoulder) [33,38].

The survival of Chinese hamster V79 cells has also been scored as a function of DNA-incorporated 125-iodine and compared with that of 131-iodine [20]. Unlike the low-LET type of survival curve (with shoulder) obtained following the decay of β-emitting 131-iodine in DNA, a high-LET curve (with no shoulder) is observed with 125-iodine, and the slope of the 125-iodine curve is much steeper than that of the 131-iodine curve. Kassis *et al.* have reported a mean relative biological effectiveness (RBE) of 7.3 when the cumulated dose to the cell nucleus at 37% survival is compared with the corresponding value from 250 kVp X-rays for the same cell line [33]. In contrast, the decay of 125-iodine in the cytoplasm, which is much less efficient at cell killing, has an RBE of ~ 1.3. Such results support the notion that the biological effects of an

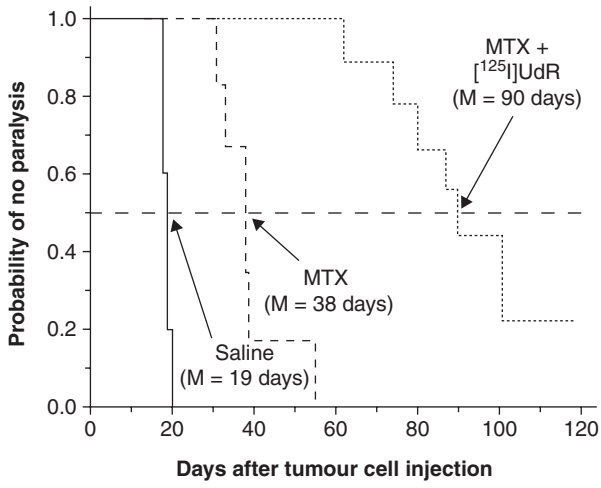

Figure 9. Induction of hind leg paralysis in rats by intrathecally growing human tumour cells after various treatment protocols. Treatments include: saline (10 µl) on days 3 – 14; methotrexate (31 µg/10 µl saline) on day 3, 5, 7, 9, 11 and 13; methotrexate (31 µg/10 µl saline) on day 3, 5, 7, 9, 11 and 13 plus (^{125}I)UdR (200 µCi/10 µl saline) on day 4, 6, 8, 10, 12 and 14.
M: Median; MTX: Methotrexate.

Auger-electron emitter are strongly dependent on its intracellular localisation, in particular its proximity to DNA.

The extreme degree of cytotoxicity observed with DNA-incorporated Auger-electron emitters has been exploited in experimental radionuclide therapy. In most of these *in vivo* studies, the thymidine analogue 5-iodo-2′-deoxyuridine (IUdR) has been used [39-42], and the results have shown excellent therapeutic efficacy. For example, the injection of [^{125}I]UdR into mice bearing an intraperitoneal ascites ovarian cancer has led to a 5-log reduction in tumour cell survival [39]. Similar findings occur with [^{123}I]UdR [40]. Therapeutic doses of [^{125}I]UdR injected intrathecally into rats with intrathecal tumours significantly delay the onset of paralysis, and the coadministration of methotrexate, an antimetabolite that enhances IUdR uptake by DNA-synthesising cells, substantially enhances the therapeutic efficacy (Figure 9) as exemplified by a 5 – 6-log tumour cell kill and the curing of ~ 30% of the tumour-bearing rats [41,42].

8. Expert opinion and conclusions

A significant increase in our understanding of the dosimetry and therapeutic potential of various modes of radioactive decay has heightened the possibility of utilising radiolabelled carriers in cancer therapy. Moreover, as a consequence of the great strides in genomics, the development of more precise targeting molecules is at hand. Further progress in the field of targeted radionuclide therapy is being made by the judicious design of radiolabelled molecules that match the physical and chemical characteristics of both the radionuclide and the carrier molecule with the clinical character of the tumour. Whereas significant improvement has been made in the treatment of highly radiosensitive haematolymphoid tumours in humans, the radionuclide therapy of solid tumours remains a challenge. In conclusion:

- If sufficient uniformity of radiopharmaceutical distribution can be achieved, α-particle and Auger-electron emitters will be practical for therapy and, in this situation, tumour size is irrelevant.
- If radiopharmaceutical distribution within the tumour is nonuniform, energetic β-particle emitters will be routinely used and, obviously, all tumour cells must be within range of the emitted particles.
- Targeted radionuclide therapy will rely increasingly on both the accessibility to various radionuclides, their availability in large quantities and at high specific activity, and the development of more specific carriers, hopefully provided by knowledge of genomics.
- Dose specification must incorporate information on nonuniformity, RBE and cellular localisation of the therapeutic radionuclide.

Acknowledgements

Financial support: this article was supported by DOE, DE-FG02-96ER62176; NIH, 5 R01 CA15523; and NIH, 5 R01 CA89648.

Bibliography

Papers of special note have been highlighted as either of interest (•) or of considerable interest (••) to readers.

1. WALICKA MA, VAIDYANATHAN G, ZALUTSKY MR, ADELSTEIN SJ, KASSIS AI: Survival and DNA damage in Chinese hamster V79 cells exposed to alpha particles emitted by DNA-incorporated astatine-211. *Radiat. Res.* (1998) 150:263-268.

• Experimental demonstration of the effects of nonuniform irradiation by α-particles on cell survival.

2. GODDU SM, HOWELL RW, RAO DV: Cellular dosimetry: absorbed fractions for monoenergetic electron and alpha particle sources and S-values for radionuclides uniformly distributed in different cell compartments. *J. Nucl. Med.* (1994) 35:303-316.

•• The tables within are essential for dose calculations at the cellular level.

3. SASTRY KSR, HOWELL RW, RAO DV *et al.*: Dosimetry of Auger emitters: physical and phenomenological approaches. In: *DNA Damage by Auger Emitters*. KF Baverstock, DE Charlton (Eds.), Taylor and Francis, London, UK (1988):27-38.

4. WRIGHT HA, HAMM RN, TURNER JE, HOWELL RW, RAO DV, SASTRY KS: Calculations of physical and chemical reactions with DNA in aqueous solution from Auger cascades. *Radiat. Prot. Dosim.* (1990) 31:59-62.

5. KASSIS AI, ADELSTEIN SJ, HAYDOCK C, SASTRY KS: Radiotoxicity of ^{75}Se and ^{35}S: theory and application to a cellular model. *Radiat. Res.* (1980) 84:407-425.

•• Methods for subcellular dosimetry.

6. KASSIS AI, ADELSTEIN SJ, HAYDOCK C, SASTRY KS, MCELVANY KD, WELCH MJ: Lethality of Auger electrons from the decay of bromine-77 in the DNA of mammalian cells. *Radiat. Res.* (1982) 90:362-373.

7. KASSIS AI, SASTRY KS, ADELSTEIN SJ: Intracellular localisation of Auger electron emitters: biophysical dosimetry. *Radiat. Prot. Dosim.* (1985) 13:233-236.

8. XUE LY, BUTLER NJ, MAKRIGIORGOS GM, ADELSTEIN SJ, KASSIS AI: Bystander effect produced by radiolabeled tumor cells *in vivo*. *Proc. Natl. Acad. Sci. USA* (2002) 99:13765-13770.

•• The first demonstration of Auger-electron-induced bystander effect in animals.

9. HUMM JL, CHIN LM, COBB L, BEGENT R: Microdosimetry in radioimmunotherapy. *Radiat. Prot. Dosim.* (1990) 31:433-436.

10. ICRU: Absorbed-dose specification in nuclear medicine (ICRU Report 67). *J. ICRU* (2002) 2(1):1-110.

• Source for absorbed doses.

11. O'DONOGHUE JA: The impact of tumor cell proliferation in radioimmunotherapy. *Cancer* (1994) 73:974-980.

12. JAIN RK: Physiological barriers to delivery of monoclonal antibodies and other macromolecules in tumors. *Cancer Res.* (1990) 50 (Suppl. 3):814s-819s.

• An excellent overview addressing the factors underlying the barriers opposing the diffusion of molecules throughout tumours.

13. NETTI PA, HAMBERG LM, BABICH JW *et al.*: Enhancement of fluid filtration across tumor vessels: implication for delivery of macromolecules. *Proc. Natl. Acad. Sci. USA* (1999) 96:3137-3142.

• Concepts relating to the diffusion of macromolecules throughout tumours.

14. KASSIS AI, HARRIS CR, ADELSTEIN SJ, RUTH TJ, LAMBRECHT R, WOLF AP: The *in vitro* radiobiology of astatine-211 decay. *Radiat. Res.* (1986) 105:27-36.

15. CHARLTON DE, KASSIS AI, ADELSTEIN SJ: A comparison of experimental and calculated survival curves for V79 cells grown as monolayers or in suspension exposed to alpha irradiation from ^{212}Bi distributed in the growth medium. *Radiat. Prot. Dosim.* (1994) 52:311-315.

16. BLOOMER WD, MCLAUGHLIN WH, LAMBRECHT RM *et al.*: ^{211}At radiocolloid therapy: further observations and comparison with radiocolloids of ^{32}P, ^{165}Dy, and ^{90}Y. *Int. J. Radiat. Oncol. Biol. Phys.* (1984) 10:341-348.

•• An excellent demonstration of the therapeutic potential of α-particles *in vivo*.

17. MACKLIS RM, KINSEY BM, KASSIS AI *et al.*: Radioimmunotherapy with alpha-particle–emitting immunoconjugates. *Science* (1988) 240:1024-1026.

18. ZALUTSKY MR, MCLENDON RE, GARG PK, ARCHER GE, SCHUSTER JM, BIGNER DD: Radioimmunotherapy of neoplastic meningitis in rats using an α-particle-emitting immunoconjugate. *Cancer Res.* (1994) 54:4719-4725.

19. MCDEVITT MR, MA D, LAI LT *et al.*: Tumor therapy with targeted atomic nanogenerators. *Science* (2001) 294:1537-1540.

20. CHAN PC, LISCO E, LISCO H, ADELSTEIN SJ: The radiotoxicity of iodine-125 in mammalian cells. II. A comparative study on cell survival and cytogenetic responses to ^{125}IUdR, ^{131}IUdR, and ^{3}HTdR. *Radiat. Res.* (1976) 67:332-343.

21. BURKI HJ, KOCH C, WOLFF S: Molecular suicide studies of ^{125}I and ^{3}H disintegration in the DNA of Chinese hamster cells. *Curr. Top. Radiat. Res. Q.* (1977) 12:408-425.

22. ESTEBAN JM, SCHLOM J, MORNEX F, COLCHER D: Radioimmunotherapy of athymic mice bearing human colon carcinomas with monoclonal antibody B72.3: histological and autoradiographic study of effects on tumors and normal organs. *Eur. J. Cancer Clin. Oncol.* (1987) 23:643-655.

23. OTTE A, MUELLER-BRAND J, DELLAS S, NITZSCHE EU, HERRMANN R, MAECKE HR: Yttrium-90-labelled somatostatin-analogue for cancer treatment. *Lancet* (1998) 351:417-418.

24. CHINN PC, LEONARD JE, ROSENBERG J, HANNA N, ANDERSON DR: Preclinical evaluation of ^{90}Y-labeled anti-CD20 monoclonal antibody for treatment of non-Hodgkin's lymphoma. *Int. J. Oncol.* (1999) 15:1017-1025.

25. AXWORTHY DB, RENO JM, HYLARIDES MD *et al.*: Cure of human carcinoma xenografts by a single dose of pretargeted yttrium-90 with negligible toxicity. *Proc. Natl. Acad. Sci. USA* (2000) 97:1802-1807.

•• An excellent demonstration of the therapeutic potential of β-particles *in vivo*.

26. DENARDO GL, KUKIS DL, SHEN S *et al.*: Efficacy and toxicity of ^{67}Cu-2IT-BAT-Lym-1 radioimmunoconjugate in mice implanted with human Burkitt's lymphoma (Raji). *Clin. Cancer Res.* (1997) 3:71-79.

27. KAMINSKI MS, ZASADNY KR, FRANCIS IR *et al.*: Radioimmunotherapy of B-cell lymphoma with [^{131}I]anti-B1 (anti-CD20) antibody. *N. Engl. J. Med.* (1993) 329:459-465.

28. WITZIG TE: Yttrium-90-ibritumomab tiuxetan radioimmunotherapy: a new treatment approach for B-cell non-Hodgkin's lymphoma. *Drugs Today* (2004) 40:111-119.

29. KAMINSKI MS, TUCK M, ESTES J *et al.*: ^{131}I-tositumomab therapy as initial treatment for follicular lymphoma. *N. Engl. J. Med.* (2005) 352:441-449.

30. KASSIS AI, ADELSTEIN SJ, HAYDOCK C, SASTRY KS: Thallium-201: an experimental and a theoretical radiobiological approach to dosimetry. *J. Nucl. Med.* (1983) 24:1164-1175.

31. KASSIS AI, SASTRY KS, ADELSTEIN SJ: Intracellular distribution and radiotoxicity of chromium-51 in mammalian cells: Auger-electron dosimetry. *J. Nucl. Med.* (1985) 26:59-67.

32. KASSIS AI, SASTRY KS, ADELSTEIN SJ: Kinetics of uptake, retention, and radiotoxicity of ^{125}IUdR in mammalian cells: implications of localized energy deposition by Auger processes. *Radiat. Res.* (1987) 109:78-89.

• Dosimetry of DNA-incorporated Auger-electron emitters.

33. KASSIS AI, FAYAD F, KINSEY BM, SASTRY KS, TAUBE RA, ADELSTEIN SJ: Radiotoxicity of ^{125}I in mammalian cells. *Radiat. Res.* (1987) 111:305-318.

34. KASSIS AI, MAKRIGIORGOS GM, ADELSTEIN SJ: Implications of radiobiological and dosimetric studies of DNA-incorporated ^{123}I: the use of the Auger effect as a biological probe at the nanometre level. *Radiat. Prot. Dosim.* (1990) 31:333-338.

• The biophysical aspects of low energy electron irradiation.

35. HOFER KG, HUGHES WL: Radiotoxicity of intranuclear tritium, ^{125}iodine and ^{131}iodine. *Radiat. Res.* (1971) 47:94-109.

36. BLOOMER WD, MCLAUGHLIN WH, WEICHSELBAUM RR *et al.*: Iodine-125-labelled tamoxifen is differentially cytotoxic to cells containing oestrogen receptors. *Int. J. Radiat. Biol.* (1980) 38:197-202.

37. WALICKA MA, DING Y, ROY AM, HARAPANHALLI RS, ADELSTEIN SJ, KASSIS AI: Cytotoxicity of [^{125}I]iodoHoechst 33342: contribution of scavengeable effects. *Int. J. Radiat. Biol.* (1999) 75:1579-1587.

38. HOFER KG, HARRIS CR, SMITH JM: Radiotoxicity of intracellular ^{67}Ga, ^{125}I and ^{3}H: nuclear versus cytoplasmic radiation effects in murine L1210 leukaemia. *Int. J. Radiat. Biol.* (1975) 28:225-241.

• The first demonstration of the marked differences in the radiotoxicity of Auger-electron irradiation when the radionuclide is localised within the cytoplasm or the nuclei of mammalian cells.

39. BLOOMER WD, ADELSTEIN SJ: 5-^{125}I-iododeoxyuridine as prototype for radionuclide therapy with Auger emitters. *Nature* (1977) 265:620-621.

•• The first demonstration of the therapeutic efficacy of Auger electrons *in vivo*.

40. BARANOWSKA-KORTYLEWICZ J, MAKRIGIORGOS GM, VAN DEN ABBEELE AD, BERMAN RM, ADELSTEIN SJ, KASSIS AI: 5-[^{123}I]iodo-2'-deoxyuridine in the radiotherapy of an early ascites tumor model. *Int. J. Radiat. Oncol. Biol. Phys.* (1991) 21:1541-1551.

41. KASSIS AI, DAHMAN BA, ADELSTEIN SJ: *In vivo* therapy of neoplastic meningitis with methotrexate and 5-[^{125}I]iodo-2′-deoxyuridine. *Acta Oncol.* (2000) 39:731-737.

42. KASSIS AI, KIRICHIAN AM, WANG K, SAFAIE SEMNANI E, ADELSTEIN SJ: Therapeutic potential of 5-[^{125}I]iodo-2'-deoxyuridine and methotrexate in the treatment of advanced neoplastic meningitis. *Int. J. Radiat. Biol.* (2004) 80:941-946.

•• An excellent demonstration of the therapeutic potential of Auger electrons in solid tumours.

Affiliation

Amin I Kassis PhD
Harvard Medical School, Department of Radiology, Armenise Building,
200 Longwood Avenue, Boston, MA 02115, USA
Tel: +1 617 432 7777; Fax: +1 617 432 2419;
E-mail: amin_kassis@hms.harvard.edu